Coulomb staircase in STM current through granular films

H. Imamura
CREST and Institute for Materials Research, Tohoku University, Sendai 980-8577, Japan

J. Chiba, S. Mitani, K. Takanashi, S. Takahashi, S. Maekawa, and H. Fujimori
Institute for Materials Research, Tohoku University, Sendai 980-8577, Japan

(Received 30 June 1999)

The tunneling current through a junction array consisting of a scanning tunneling microscope tip and a granular film is studied both theoretically and experimentally. When the tunnel resistance between the tip and a granule on the surface is much larger than those between granules, a bottleneck of the tunneling current is created in the array and the Coulomb staircase (CS) appears in the *I-V* curve at room temperature. It is shown that the period of the CS is given by the capacitance at the bottleneck even though a granular film consists of many tunnel junctions with different capacitances. Our study provides a possibility for single-electron-spin-electronic devices at room temperature.

Charging effects on single-electron tunneling such as Coulomb blockade and Coulomb oscillation have attracted much interest.[1] The scanning tunneling microscope (STM) is a good tool to investigate the charging effects. Recently, the steplike structure called the Coulomb staircase (CS) is observed in the *I-V* curve by using an STM tip of nanometer size in highly resistive granular films[2–5] as well as in metal-droplet systems.[6,7] The *I-V* characteristics for double tunnel junction systems have been extensively studied and the CS is observed when the resistances between the junctions are not equal.[1,8] For these asymmetric double junction systems, the junction with a large resistance behaves like a bottleneck of the tunneling current and the central island is charged through the other junction up to the maximum charge. The tunneling current jumps when the charge changes.

However, the physics behind the CS in a granular film is not clear because it contains many granules with different size and the conducting path may form a three-dimensional network in a thick granular film. Bar-Sadeh *et al*. have studied the STM current through a nonmagnetic granular film, Au-Al_2O_3, by using the cryogenic STM.[2,3] They observed the CS at temperatures $T=4.2$ and 78 K, and analyzed the experimental data by using a triple barrier model. They assumed that the rate for tunneling between two granules is small and the number of excess electrons in each granule is treated independently. Because of these assumptions, the CS was given by the superposition of two different periods in their model: one was determined by the tunnel process between the STM tip and a granule, the other between another granule and the base electrode. On the contrary, as we will show later, the CS has a single period which is determined by the capacitance at the bottleneck.

In this paper, we study the STM current through a granular film both theoretically and experimentally. In this system, we can vary the tunnel resistance between the tip and a granule on the surface by changing the distance between them. When the tunnel resistance between the tip and a granule on the surface is much larger than those between granules, a bottleneck of the tunneling current is created in the array. Theoretically, we find that the period of the CS is given by the capacitance of the bottleneck even in a thick film with many granules between the tip and the base electrode. We present results from STM experiments on 10-nm and 1-μm-thick Co-Al-O granular films which have the CS with a single period at room temperature. We propose that tunnel magnetoresistance (TMR) oscillates with the same period as the CS for magnetic granular films. Our theoretical and experimental studies provide a direction for single-electron-spin-electronic devices at room temperature.

Our setup is schematically shown in Figs. 1(a) and 1(b). The current flows from the STM tip to the base electrode through a granular film. The system with a thin granular film in panel (a) is modeled by the one-dimensional array of tunnel junctions as in panel (c). We will show that our experimental results for the 10-nm-thick film are well explained by this model with $N=3$. On the other hand, such a one-

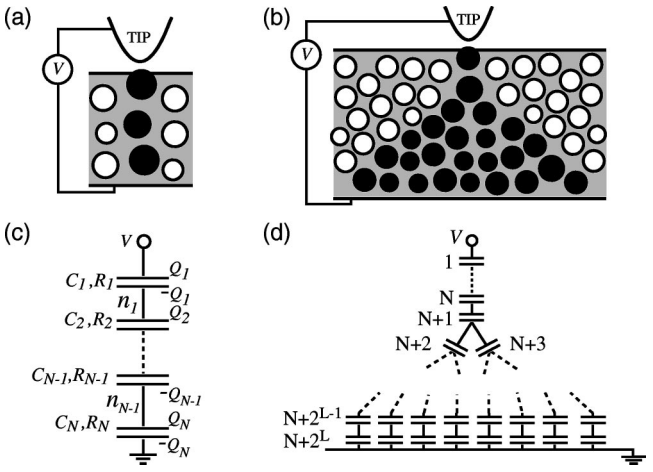

FIG. 1. The system with an STM tip and a thin (thick) granular film is schematically shown in panel (a) [(b)]. Filled (hollow) circles represent granules in (out of) the conducting path. The insulating matrix is indicated by the shading. The corresponding theoretical models for (a) and (b) are shown in panels (c) and (d), respectively. For the thick film, a Bethe-lattice network of granules, where each granule has three neighbors, is connected to the one-dimensional array.

dimensional array is not appropriate for a thick granular film, because, as illustrated in Fig. 1(b), the conducting paths spread and form a three-dimensional network as the distance from the tip increases. We model this system by a one-dimensional array of N junctions connected to a Bethe-lattice network with three nearest neighbors as shown in Fig. 1(d). Each junction is characterized by a tunnel resistance R_j, capacitance C_j, and carrying charge Q_j. The number of excess electrons in the kth granule is represented by n_k.

The free energy for the state characterized by the set of charges $\{n_i\}\equiv(n_1,n_2,\ldots)$ is given by

$$F(\{n_i\})=\sum_i \frac{Q_i^2}{2C_i}-(Q_1-e\xi)V, \tag{1}$$

where Q_1 represents the charge at the granule on the surface, ξ is the number of electrons supplied by the voltage source, and i goes from 1 to N. When an electron tunnels through the kth junction, the charge Q_i deviates from its initial value by δQ_i^k. Let us consider the energy change due to the single-electron tunneling, $E_k^{\pm}$, where the superscript $+$ $(-)$ denotes the process that an electron tunnels upward (downward) through the kth junction in Figs. 1(c) and 1(d). In order to investigate the mechanism of the CS, we have to express $E_k^{\pm}$ by using n_i instead of Q_i. After some algebra, we obtain the energy change $E_k^{\pm}$ for both junction arrays shown in Figs. 1(c) and 1(d):

$$E_k^{\pm}(\{n_i\})=\sum_i \left(\widetilde{\sum_{j<i}}\frac{\delta Q_j^k}{C_j}\right)n_i+\frac{1}{2}\sum_i\frac{(\delta Q_i^k)^2}{C_i} -(\delta Q_1^k\pm e\,\delta_{1,k})V, \tag{2}$$

where $\widetilde{\Sigma}_i$ represents the summation along the conducting path, and $\delta_{1,k}$ is Kronecker's delta function. The deviation δQ_i^k is determined by Kirchhoff's law and is independent of the number of excess electrons $\{n_i\}$. The tunneling rate is obtained by using the golden rule[1] as

$$\Gamma_k^{\pm}(\{n_i\})=\frac{E_k^{\pm}(\{n_i\})}{e^2R_k[\exp(E_k^{\pm}(\{n_i\})/T)-1]}. \tag{3}$$

By solving the master equation for the probability of states $p(\{n_i\})$,[1] the tunneling current through the kth junction is obtained as

$$I_k=e\sum_{\{n_i\}}p(\{n_i\})[\Gamma_k^+(\{n_i\})-\Gamma_k^-(\{n_i\})]. \tag{4}$$

For simplicity, we neglect the effect of residual fractional charge,[2,3,8] cotunneling,[9–11] spin accumulation,[12–14] and level quantization[15] in the granules.

We first look at the I-V characteristics for a one-dimensional array of tunnel junctions with a bottleneck of the tunneling current between the tip and a granule on the surface. In Figs. 2(a) and 2(b), we present the numerical results for tunnel junctions with $N=2-5$ at $T=0$, N being the number of junctions. Due to the charging energy in each junction, single-electron tunneling is blocked as long as the bias voltage V is lower than the threshold value V_T.[16] From Eq. (2) the bias voltage V_T^k, above which the initial state $(0,\ldots,0)$ is unstable for electron tunneling through kth junction, i.e., $E_k^+(0,\ldots,0)<0$, is given by

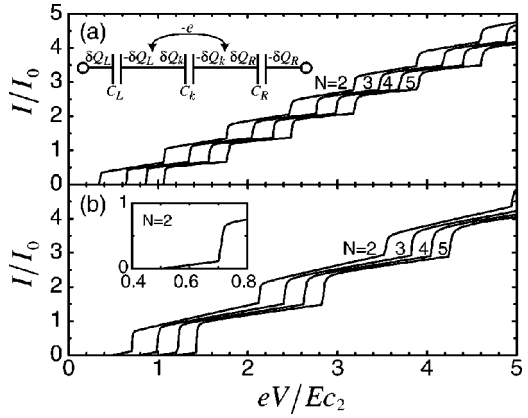

FIG. 2. The tunneling current normalized with $I_0=E_{C_2}/eR_1$, where $E_{C_2}=e^2/C_2$, is plotted against the bias voltage at $T=0$. The number of junctions are $N=2-5$ from left to right. The tunnel resistance ratio is taken to be $R_1:R_2:R_3:R_4:R_5=1000:1:1:1:1$. The capacitance ratio is (a) $C_1:C_2:C_3:C_4:C_5=\sqrt{2}:1:\sqrt{3}:\sqrt{5}:\sqrt{6}$, (b) $C_1:C_2:C_3:C_4:C_5=1/\sqrt{2}:1:\sqrt{3}:\sqrt{5}:\sqrt{6}$. The tunneling current with $n_1=0$ as a dominant state for $N=2$ is shown in the inset of panel (b).

$$V_T^k=\frac{\sum_i(\delta Q_i^k)^2/C_i}{2(\delta Q_1^k+e\,\delta_{1,k})}=\frac{e}{2}\left(\frac{1}{C_T}-\frac{1}{C_k}\right). \tag{5}$$

The last expression in Eq. (5) is obtained by considering the equivalent network shown in the inset of Fig. 2(a), where $1/C_L=\Sigma_{i<k}1/C_i$ and $1/C_R=\Sigma_{i>k}1/C_i$. The threshold voltage is given by $V_T=\min_k V_T^k$. As pointed out by Melsen *et al.*, the Coulomb blockade region increases as the number of junctions, N, increases[16] as shown in Figs. 2(a) and 2(b). For large N, the threshold voltage is expressed in terms of the average capacitance $\langle C\rangle$ as $V_T\simeq(e/2\langle C\rangle)(N-1)$ and is proportional to the film thickness, because the total capacitance is inversely proportional to the layer thickness.

For a thick film with many granules between the tip and the base electrode, the conducting paths form a three-dimensional network as shown in Figs. 1(b) and 1(d). The decrease of the total capacitance for a junction network with increasing film thickness is much weaker than that for a one-dimensional array. Therefore, the threshold voltage V_T of a thick film remains of the same order of magnitude as that for a thin film. Later we will show that the experimental results for 1 μm-thick film are well explained by considering the junction network as the Bethe lattice as shown in Fig. 1(d).

The CS is classified into two types as shown in Figs. 2(a) and 2(b). The criterion is whether the capacitance C_1 of the bottleneck is the smallest of all of the junctions, i.e., whether $V_T=V_T^1$ or $V_T=\min_{k\neq1}V_T^k$. A typical CS for $V_T=\min_{k\neq1}V_T^k$ is given in Fig. 2(a), where electrons start to accumulate at the bottleneck once the bias voltage exceeds V_T. Until the accumulated electrons tunnel out through the bottleneck, the voltage drop caused by them forbids electrons to tunnel through the other junctions. Therefore, the stable state is given by $(n_1,0,\ldots,0)$ and the tunneling current jumps at the

bias voltage where the number of accumulated electrons n_1 changes. This number n_1 is the minimum value satisfying the conditions

$$E_1^+(n_1,0,\ldots,0)<0, \quad E_{k\neq 1}^+(n_1,0,\ldots,0)\geqslant 0. \tag{6}$$

The first condition represents that accumulated electrons tunnel out through the first junction. The second indicates that electrons cannot tunnel through the other junctions, and is rewritten as $(e^2/C_1)n_1 \geqslant eV - V_T^{k\neq 1}$. Therefore, the tunneling current jumps at the bias voltage V given by

$$V=\min_{k\neq 1} V_T^k + (e^2/C_1)(n_1-1). \tag{7}$$

From Eq. (7), one can easily see that the CS has a single period of e/C_1. The tunneling current for each plateau of the CS is approximately given by $I \simeq e\Gamma_1^+(n_1,0,\ldots,0)$.

On the other hand, if C_1 is the smallest, the tunneling current does not jump at V_T as shown in Fig. 2(b). For $V_T < V < \min_{k\neq 1} V_T^k$, the tunneling current is approximately given by $I \simeq e\Gamma_1^+(0,\ldots,0)$. Once V exceeds $\min_{k\neq 1} V_T^k$, electrons start to accumulate at the bottleneck and the I-V curve shows a CS. The bias voltage V at which the tunneling current jumps is given by Eq. (7).[17]

When the bottleneck is placed at another junction $j(1<j<N)$, the stable state is $(0,\ldots,0,n_{j-1}=-n_j,n_j,0,\ldots,0)$ and the period of the CS is determined by the capacitance C_j at the bottleneck. The CS is classified into two types in the same way as those shown in Figs. 2(a) and 2(b). However, the criterion is whether the capacitance C_j is the smallest or not.

The period of CS in a thick film shown in Figs. 1(b) and 1(d) is also determined from Eqs. (2) and (6), as long as the tip is coupled to a single granule on the surface and the bottleneck is created between them. Therefore, the voltage where the tunneling current jumps is given by Eq. (7). The CS has a single period determined by the capacitance at the bottleneck, even for a thick film.

We have performed STM experiments on Co-Al-O granular films. Samples with different thicknesses were prepared by an oxygen-reactive sputtering with a Co-Al alloy target; 10-nm- and 1-μm-thick $Co_{36}Al_{22}O_{42}$ films consisting of Co granules embedded in an Al-oxide matrix were deposited on glass substrates. For the 10-nm-thick $Co_{36}Al_{22}O_{42}$ film, a 200-nm-thick Co-Al alloy layer was inserted between the Co-Al-O granular film and the glass substrate as a base electrode. A conventional STM system (DME, Rasterscope 3000) with a Pt tip was operated at room temperature under high vacuum ($\sim 10^{-8}$ Torr). We have obtained clear topographic images consistent with the TEM observations where nm-sized Co granules are embedded in an Al-oxide matrix.[5] The I-V curves were obtained by placing the tip on a Co granule. The tunnel resistance between granules for Co-Al-O granular films is estimated to be 10^5–10^6 Ω from the average diameter of granules (~ 3 nm), the average intergranular distance (~ 1 nm), and electrical resistivity.[5,10] On the other hand, the tunnel resistance between the tip and a granule on the surface, R_1, is 10^8–10^9 Ω. Therefore, R_1 is 10^2–10^4 times larger than the other tunnel resistances. Surface effects such as contaminates, oxide barriers and a layer of water molecules can be renormalized in the capacitance C_1 and the resistance R_1 at the first junction.

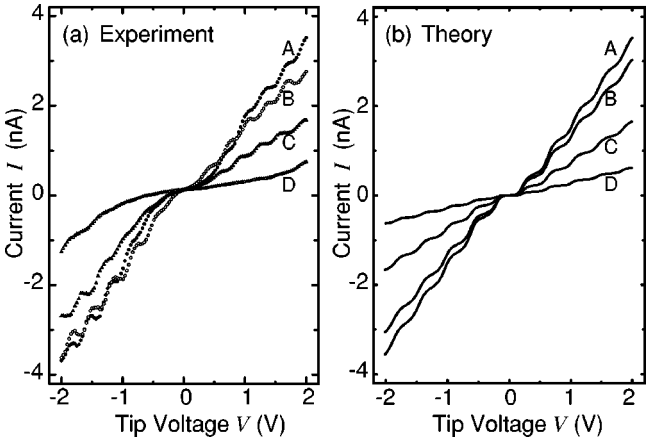

FIG. 3. (a) Experimental I-V curves for a 10-nm-thick $Co_{36}Al_{22}O_{42}$ at room temperature. A, B, C, and D refer to different distances between the STM tip from the surface of the sample. The lateral position for A and B is different from that for C and D. (b) Corresponding theoretical curves in a triple tunnel junction system at $T=300$ K. The tunnel resistance at the bottleneck is taken to be $R_1=600$, 700, 1300, and 3500 MΩ for lines A, B, C, and D, respectively. The other tunnel resistances are $R_2=R_3=1$ MΩ and the capacitances are $C_1=4.48\times10^{-19}$ F, $C_2=2.13\times10^{-19}$ F, and $C_3=3.62\times10^{-19}$ F for all curves.

The experimental I-V curves for a 10-nm-thick $Co_{36}Al_{22}O_{42}$ film are plotted in Fig. 3 (a). There exist two or three granules between the tip and base electrode. Even at room temperature, the tunneling current shows a clear CS with a single period. The I-V curves for a 1-μm-thick $Co_{36}Al_{22}O_{42}$ film are plotted in Fig. 4(a). We also find the CS with a single period. Note that for this thick film, 200 to 300 Co granules exist in the direction perpendicular to the film plane between the tip and the substrate. Let us now analyze our experimental results by using the theory presented above.

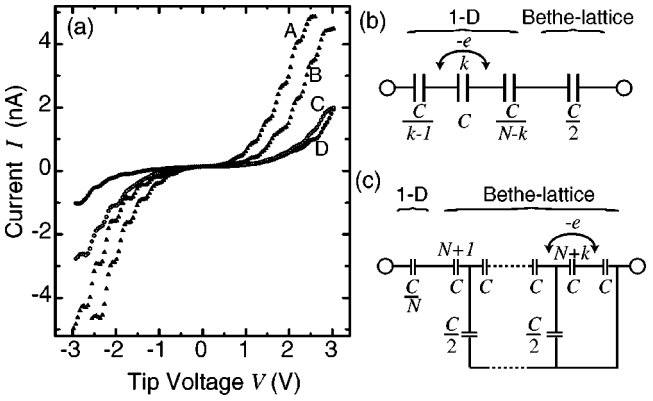

FIG. 4. (a) Experimental I-V curves for a 1-μm-thick $Co_{36}Al_{22}O_{42}$ film at room temperature. A, B, C, and D refer to different distances of the STM tip from the surface of the sample. The lateral tip position for A and B is different from that for C and D. (b) The equivalent network for the electron tunneling in the one-dimensional array, where the Bethe-lattice network is replaced by its total capacitance $C/2$. (c) The equivalent network for the electron tunneling in the Bethe-lattice network.

We first examine the I-V curves for the 10-nm-thick film. A triple tunnel junction model with a bottleneck between the tip and a granule on the surface is used for the calculation. The calculated I-V curves are shown in Fig. 3(b). Parameter values were chosen in the ranges estimated from the experiments. We find that the theoretical curves explain the experimental ones very well.

For the thick film, on the other hand, the conducting paths are considered to form a three-dimensional network inside the film; this is a more complicated system compared to the thin granular films for which the CS was observed so far.[2–4] The value of the threshold voltage $V_T \simeq 0.5$ V is not explained by the one-dimensional array model, because the threshold voltage V_T is proportional to the layer thickness in this model and is about 100 times larger than that for 10-nm-thick film; this is in contrast with the experimental data.

As mentioned before, this discrepancy can be resolved by considering a network of the conducting paths. We describe the thick film as a one-dimensional array connected to a Bethe-lattice network as shown in Fig. 1(d). The bottleneck is created between the tip and a granule on the surface. Therefore, the stable states are given by $(n_1,0,\ldots,0)$ and the tunneling current jumps when the number of accumulated electrons n_1 changes. The voltage where the current jumps is given by Eq. (7) and the CS has a single period of e/C_1 even for a thick film. The equivalent network to obtain the threshold voltage for kth junction V_T^k is shown in Figs. 4(b) and 4(c), where we assume, for simplicity, the same capacitance C for all junctions. The key point is that for electron tunneling in the one-dimensional array, the Bethe-lattice network is replaced by its total capacitance as shown in Fig. 4(b). The total capacitance for the Bethe lattice is $C/2$ and the bias voltage V at which the tunneling current jumps [see Eq. (7)] is given by $V=(e/2C)(N+1)+(e/C)(n_1-1)$. The experimental results shown in Fig. 4(a) are consistent with our model with $N \simeq 2$.

The TMR in tunnel junctions with ferromagnetic electrodes[18,19] and magnetic granular films[10] is another attractive topic. Recently, the TMR oscillations in asymmetric double tunnel junctions with ferromagnetic electrodes have been studied.[20,21] The condition for TMR oscillations is that the tunneling current shows the CS and the magnetic field dependence of the tunnel resistance is not the same for all tunnel junctions. The TMR oscillations with the same period as the CS may be observed for magnetic granular films. Our calculation shows that the amplitude of the TMR oscillation is about 5% at room temperature for the curve A in Fig. 3(b).

In summary, the electron transport through an array of tunnel junctions consisting of an STM tip and a granular film has been studied both theoretically and experimentally. When the tunnel resistance between the tip and a granule on the surface is much larger than those between granules, a bottleneck is created in the array and a CS with a single period is observed in the I-V curve. We predicted that the period of the CS is given by the capacitance at the bottleneck even in a thick film with many granules between the tip and the base electrode. Our STM experiments on 10-nm- and 1-μm-thick Co-Al-O granular films confirmed the CS with a single period at room temperature. TMR oscillations for magnetic granular films are also predicted. Our theoretical and experimental studies provide a direction for single-electron-spin-electronic devices at room temperature.

We thank P. M. Levy for reading the manuscript. This work was supported by a Grant-in-Aid from Scientific Research Priority Area for Ministry of Education, Science, Sports and Culture of Japan, a Grant from the Japan Society for Promotion of Science, and NEDO Japan.

[1] *Single Charge Tunneling*, edited by H. Grabert and M. H. Devoret (Plenum Press, New York, 1992).
[2] E. Bar-Sadeh *et al.*, Phys. Rev. B **50**, 8961 (1994).
[3] E. Bar-Sadeh *et al.*, J. Vac. Sci. Technol. B **13**, 1084 (1995).
[4] R. Desmicht *et al.*, Appl. Phys. Lett. **72**, 386 (1998).
[5] J. Chiba *et al.*, J. Magn. Soc. Jpn. **23**, 82 (1999).
[6] R. Wilkins, E. Ben-Jacob, and R. C. Jaklevic, Phys. Rev. Lett. **63**, 801 (1989).
[7] M. Amman, S. B. Field, and R. C. Jaklevic, Phys. Rev. B **48**, 12 104 (1993).
[8] A. E. Hanna and M. Tinkham, Phys. Rev. B **44**, 5919 (1991).
[9] S. Takahashi and S. Maekawa, Phys. Rev. Lett. **80**, 1758 (1998).
[10] S. Mitani *et al.*, Phys. Rev. Lett. **81**, 2799 (1998).
[11] D. V. Averin and Y. V. Nazarov, Phys. Rev. Lett. **65**, 2446 (1990).
[12] M. Johnson, Phys. Rev. Lett. **70**, 2142 (1995).
[13] H. Imamura, S. Takahashi, and S. Maekawa, Phys. Rev. B **59**, 6017 (1999).
[14] S. Takahashi, H. Imamura, and S. Maekawa, Phys. Rev. Lett. **82**, 3911 (1999).
[15] R. Kubo, J. Phys. Soc. Jpn. **17**, 975 (1962).
[16] J. A. Melsen *et al.*, Phys. Rev. B **55**, 10 638 (1997).
[17] For a double junction system, our classification of the CS is consistent with the results in Ref. 8.
[18] M. Julliere, Phys. Lett. **8**, 225 (1975).
[19] S. Maekawa and U. Gäfvert, IEEE Trans. Magn. **18**, 707 (1982).
[20] J. Barnaś and A. Fert, Phys. Rev. Lett. **80**, 1058 (1998).
[21] K. Majumdar and S. Hershfield, Phys. Rev. B **57**, 11 521 (1998).